

## THE ROLE OF NATURAL VARIABILITY AND ANTHROPOGENIC CLIMATE CHANGE IN THE 2017/18 TASMAN SEA MARINE HEATWAVE

S. E. PERKINS-KIRKPATRICK, A. D. KING, E. A. COUGNON, M. R. GROSE, E. C. J. OLIVER,  
N. J. HOLBROOK, S. C. LEWIS, AND F. POURASGHAR

This document is a supplement to “The Role of Natural Variability and Anthropogenic Climate Change in the 2017/18 Tasman Sea Marine Heatwave,” by S. E. Perkins-Kirkpatrick, A. D. King, E. A. Cougnon, M. R. Grose, E. C. J. Oliver, N. J. Holbrook, S. C. Lewis, and F. Pourasghar (*Bull. Amer. Meteor. Soc.*, **100**, S105–S110) • ©2019 American Meteorological Society • Corresponding author: Sarah Perkins-Kirkpatrick, sarah.kirkpatrick@unsw.edu.au • DOI:10.1175/BAMS-D-18-0116.2

**CLIMATE MODELS.** The Community Earth System Model (CESM) large ensemble provides 34 ensemble members over historical and RCP8.5 scenarios (Taylor et al. 2012), which differ only in their initial conditions [for further details, see Kay et al. (2015)]. Historical and RCP8.5 simulations were concatenated for each member, resulting in “ALL” forcing simulations spanning 1920–2100. The corresponding 1800-yr preindustrial control run was used to represent the “NAT” world. The distributions of MSLP and TS (see main text) were compared to NCEP Reanalysis 1 via the Kolmogorov–Smirnov test over 1982–2005. No significant differences were found for each simulation at a significance level of 5%.

The CMIP5 analysis was performed on the models listed in Table ES1. Models were evaluated against NCEP SST and MSLP series (Lewis and Karoly 2013). Eight models passed and were used in the analysis. The natural world is represented using HistoricalNat simulations for 1901–2005 with the “current” world represented with RCP8.5 simulations from 2008–27. A “future” high-emissions scenario was examined for the period 2041–60 in RCP8.5 simulations.

The Tasman Sea MHW was explored in 1.5° and 2°C worlds above preindustrial values, the target

global warming levels set out in the Paris Agreement (King et al. 2017). This involved selecting model years within decades when the global-average temperature was found to be close to 1.5° and 2°C (allowing 0.2°C leeway on either side) in simulations of all future climates (RCP2.6, RCP4.5, RCP6.0, and RCP8.5) above the 1901–2005 historicalNat global-average temperature (akin to a preindustrial baseline with relatively few major volcanic eruptions) for each of the same models. For a fuller explanation of this method and the sensitivity tests that were performed please see King et al. (2017). The timing of model years under each projection scenario contributing to the 1.5° and 2°C worlds is displayed in Fig. S1 of King et al. (2017).

**BLOCKING INDEX.** The Bureau of Meteorology blocking index (Pook and Gibson 1999) is a measure of atmospheric blocking tailored specifically to eastern Australia, making it particularly useful for this analysis. Blocks are defined by high surface pressure and by a split of the westerly current at 500 hPa into two branches. The index quantifies the difference between the zonal wind at the 500-hPa level at the latitude of the two branches (25°–30°S and 55°–60°S) and the latitude of the block (40°–50°S). The index was used to examine

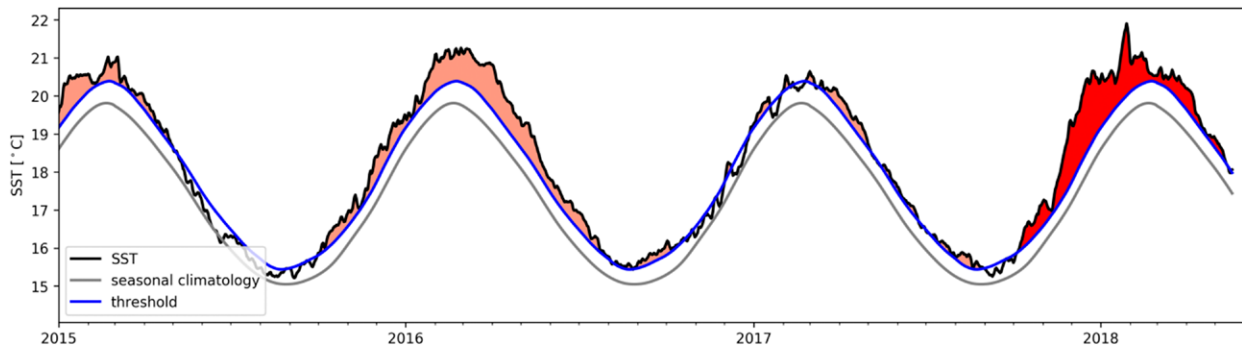


**FIG. ES1. SST time series (black) area-averaged for the Tasman Sea region using the NOAA OI SST v2 dataset. The climatology (gray) is calculated as described in the text with a baseline 1961–90 climatological period. The threshold (blue) is defined using the seasonally varying 90th percentile of daily SSTs (within an 11-day window centered on each day of year). The shading highlights marine heatwave events in the time series, with the dark red specifically highlighting the 2017/18 event focused on in this study.**

the high monthly pressure anomaly through persistent blocking. We only applied it to CESM and not CMIP5 (see below) due to concerns with the computation of the index from multiple levels across models with data interpolated onto those levels.

**COMPARISON OF 2015/2016 AND 2017/2018 TASMAN SEA MARINE HEATWAVES.** The SST time series area-averaged for the Tasman Sea region (Fig. ES1) shows a very strong increase in SST in November, coinciding with the widespread atmospheric heatwave covering the same region. Additionally, several warm core (anticyclonic) eddies were present in the region close to southeast Australia at this time and may have played a role in intensifying and/or sustaining the warming in that region, but could not explain the widespread warming for the entire Tasman Sea alone. Oliver et al. (2018b) have shown that anticyclonic (warm) eddies off the east and southeast coasts of Tasmania play an important role in driving MHW events along the southeast Australian coast.

The MSLP during the two events was similar. However, these events are substantially different. The findings of Oliver et al. (2017) demonstrate that the 2015/16 event was due to intensified heat advection (transport) in the East Australian Current (EAC) Extension in the upper ocean. The patterns seen in Fig. 1a from Oliver et al. (2017) and Fig. 1a in the present manuscript illustrate the different nature of both events, first highlighted by the far greater areal extent of the 2017/18 event. Analysis of the daily SST maps for the southeast Australia region (where EAC pulses can be observed when present) do not show as clear a signature of the EAC Extension during the 2017/18 event compared to the 2015/16 event. Furthermore, the very rapid onset and widespread development of the warming around Tasmania is consistent with

the response to large-scale local air–sea heat fluxes, and coincident with the atmospheric heatwave that occurred at the time.

We note a significant difference in the role of local air–sea heat fluxes between the 2015/16 and 2017/18 MHW events. The depth-averaged heating rate ( $^{\circ}\text{C s}^{-1}$ ) in the mixed-layer of depth  $H$  due to air–sea heat fluxes  $Q_s$  (positive into the ocean) is given by  $Q_s/(\rho_0 C_p H)$ , where  $\rho_0$  is the average seawater density ( $1024 \text{ kg m}^{-3}$ ) and  $C_p$  is the specific heat of seawater ( $4190 \text{ kg}^{-1} \text{ }^{\circ}\text{C}^{-1}$ ; e.g., Chen et al. 2014). This heating rate is proportional to  $Q_s$  and inversely proportional to  $H$ . Monthly-mean mixed-layer depths and net surface heat fluxes (including the relaxation terms and all relevant components, shortwave and longwave and latent and sensible heat fluxes) were obtained from January 1980 to April 2018 from the NCEP Global Ocean Data Assimilation System (GODAS) and were area-averaged over the domain outlined in the manuscript ( $135^{\circ}$ – $174^{\circ}\text{E}$ ,  $26^{\circ}$ – $46^{\circ}\text{S}$ ). The November to January mean values are shown below (Fig. ES2).

Mixed-layer depths were the shallowest on record (since 1980) during November–January (NDJ) 2017/18 whereas they were near average during NDJ 2015/16 (Fig. ES2, top panel). Surface heat fluxes were near average for both periods (Fig. ES2, middle panel). Therefore, we would expect a typical climatological warming of the mixed layer for NDJ 2017/18 but greater than climatological warming in 2017/18, due to the shallower layer over which the solar energy is distributed. Indeed, if we calculate the depth-averaged mixed-layer warming over the 3-month NDJ period using the equation above (integrated over 3 months) and the values of  $Q_s$  and  $H$  from GODAS we find a near-average warming in 2015/16, but the second-highest warming on record for 2017/18 (Fig. ES2, bottom panel).

**TABLE ES1. The models used in this analysis. Models listed in bold passed the evaluation test described in the paper and were used in the attribution step. Numbers refer to the simulation number per model.**

Model	Historical	HistoricalNat	RCP2.6	RCP4.5	RCP6.0	RCP8.5
Time period	(1901–2005)	(1901–2005)	(2006–2100)			
<b>ACCESS1.3</b>	1,2,3					
<b>BCC-CSM1.1</b>	1,2,3					
CanESM2	1,2,3,4,5	1,2,3,4,5	1,2,3,4,5	1,2,3,4,5		1,2,3,4,5
CCSM4	1,2,3,4,5,6	1,2,4,6	1,2,4,6	1,2,4,6	1,2,4,6	1,2,4,6
CESM1-CAM5	1,2,3	1,2,3	1,2,3	1,2,3	1,2,3	1,2,3
<b>CNRM-CM5</b>	1,2,3,4,5,6,7,8,9,10	1,2,4				1,2,4
<b>CSIRO Mk3.6.0</b>	1,2,3,4,5,6,7,8,9,10	1,2,3,4,5	1,2,3,4,5	1,2,3,4,5	1,2,3,4,5	1,2,3,4,5
<b>GFDL CM3</b>	1,2,3,4,5					
GISS-E2-H	1,2,3,4,5	1,2		1,2		1,2
GISS-E2-R	1,2,3	1,2		1,2		1,2
<b>HadGEM2-ES</b>	1,2,3,4,5	1,2,3,4	1,2,3,4	1,2,3,4	2,3,4	1,2,3,4
IPSL-CM5A-LR	1,2,3,4,5,6	1,2,3	1,2,3	1,2,3		1,2,3
IPSL-CM5A-MR	1,2,3					
<b>MIROC-ESM</b>	1,2,3					
<b>MRI-CGCM3</b>	1,2,3					
NorESM1-M	1,2,3					

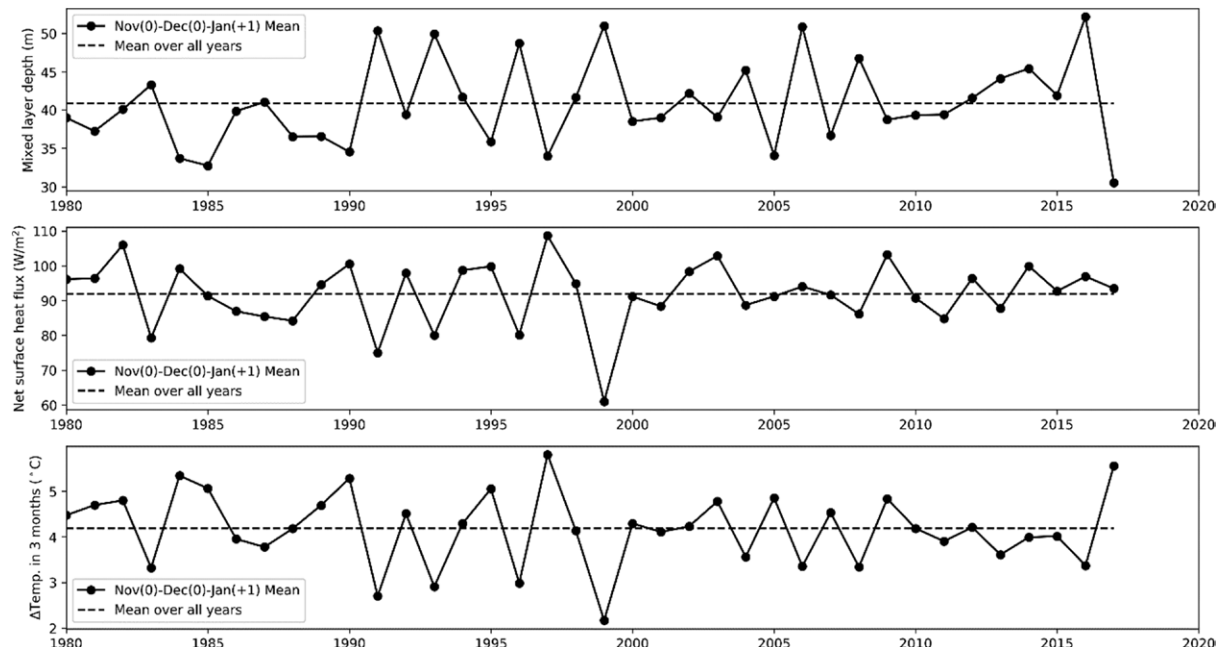


**FIG. ES2. Time series of the regionally averaged November–January (NDJ) (top) mixed-layer depth, (middle) net surface heat flux, and (bottom) depth-averaged mixed-layer warming over the 3-month NDJ period (using the equation given in the text integrated over 3 months). The data are based on the monthly mean from the NCEP Global Ocean Data Assimilation System (GODAS) from January 1980 to April 2018**